ECE 533 "Digital Imaging Processing" Course Project Report:

Despeckle Filtering in Medical Ultrasound Imaging

Hairong Shi [1]   Xingxing Wu [2]

(1) Department of Medical Physics, University of Wisconsin-Madison
(2) Department of Electrical and Computer Engineering, University of Wisconsin-Madison

Dec. 12, 2003

Percentage of each person's work:

Hairong Shi: 50%
  (Wiener Filter Method, Anisotropic Diffusion Method, Simulation of inclusion phantoms)

Xingxing Wu: 50%
  (Wavelet Filter Method, K-distribution based Adaptive Filtering Method)

I Introduction

The medical Ultrasound B-scan (brightness scan) echo imaging is acquired by summation of the echo signals from ultrasound scatterers in the ultrasound beam range. The scatterers are from structures, tissue interfaces and tissue microstructures etc. in the body, these scatterers are locally correlated. And the coherent summation of signals include the structures and interfaces information which are useful for diagnosis purpose, as well as some locally correlated multiplicative noises from scatterers smaller than ultrasound beam wavelength (resolution size), which corrupts medical ultrasound imaging and makes visual observation difficult. These noises are commonly called "**speckles**".

Even though in some cases the speckle are essential information to track features, many cases the speckle noise deteriorates the image quality, degrades the fine details and edge definition. It also limits the contrast resolution, limiting the detectability of small, low contrast lesions in body. Speckle is always considered as a primary source of medical ultrasound imaging noise, and it should be filtered out.

A simple example is shown in Fig. 1 to demonstrate the impact of speckle noise on information content (image from Duke University). The object of interest is a hypoechoic lesion of 5 mm diameter with -9 dB contrast. The echogenicity map corresponding to this object is shown in the top left panel of Fig.1. The scattering function represents the population of sub-resolution scatterers being imaged, which is shown in the top right panel of Fig. 1. The RF echo data is shown in the lower left panel. It is zero-mean and thus does not show a map of local echo magnitude. The low right panel shows the envelope detected image, which produces the desired image of echo magnitude. From the images, it is easy to see how speckle noise obscures the information in the image.

Usually in clinical application, the B-mode images shown on ultrasound machine monitor are logarithm compressed envelope-detected image, as shown in the bottom right image shown in Fig. 1. While for research application, usually Radio-frequency (RF) data are collected directly from ultrasound machine, which can be considered as "raw" data from transducer and amplifier circuits. To convert RF data into B-mode images, the data are first Hilbert transformed to detect envelope, and then do logarithm. Due to such operation, the multiplicative speckle is converted into additive noise after logarithm compression, and the signal created has a Rayleigh amplitude PDF:

$$p_A(a) = \frac{a}{\sigma^2} \exp\left(-\frac{a^2}{2\sigma^2}\right), \ a > 0$$

For images with speckles, removing speckles while not affecting important features is the purpose of despeckle. Many methods are proposed to alleviate the speckles. Spatial compounding method attempts to reduce the noise by averaging several images (Li and O'Donnell 1994). Filtering methods are practical alternatives. In this project, we implemented and tested several despeckle filters.
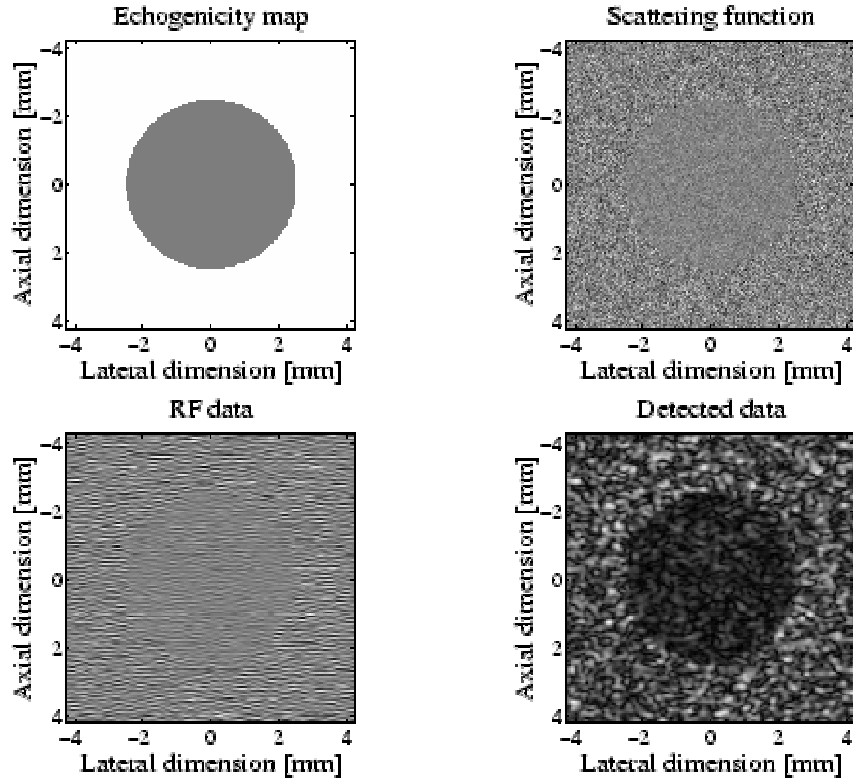
Figure 1. The ultrasound image of a hypoechoic lesion of 5 mm diameter with -9 dB contrast. **(Top Left)** The echogenicity map. **(Top Right)** The scattering function. **(Lower Left)** RF echo data. **(Lower Right)** Envelope detection Image.

## II Methods and Results

(0) Test images

In this project, we use the following figures to test our filters.

(A) 4 simulated inclusion phantoms with different contrast. The simulation program is based on a previous research in our laboratory (Li and Zagzebski, 1999). The simulated ultrasound beam has center frequency 3MHz, band width 40%, no attenuation. We simulate phantom with three different size inclusions embedded in the background gelatin, the signal contrast (inclusion to background) for four phantoms are 10dB, 5dB, -5dB and -10dB respectively. The images of these 4 phantoms are shown below.
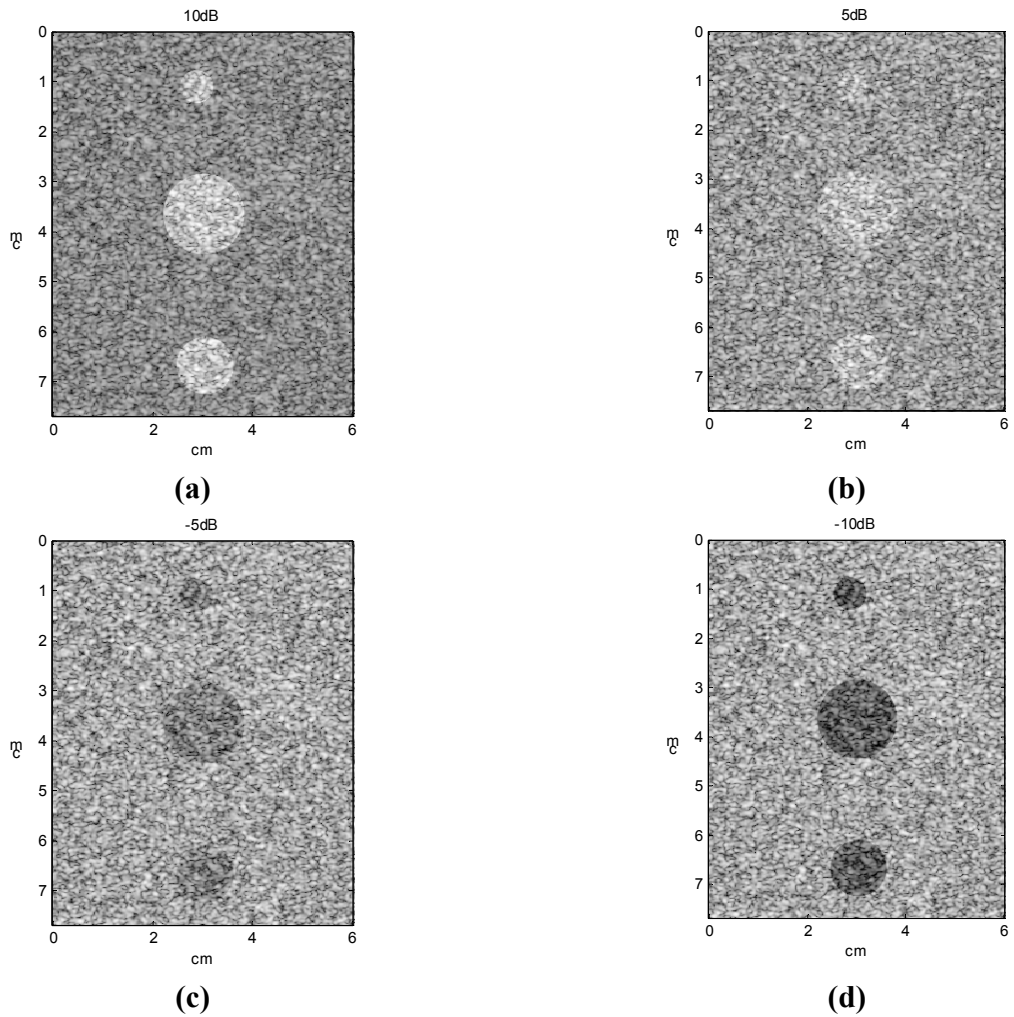
Figure 2 Four simulated phantoms with different contrast **(a)** 10dB, **(b)** 5dB, **(c)** -5dB, **(d)** -10dB

(B) We acquired RF data of a uterine phantom from Aloka SSD2000 Medical Ultrasound System. The transducer is a linear transducer with center frequency 7.5MHz, sampling rate is 100MHz, the image then is down sampled to reduce the computation time. The phantom shown has a uterine tube and three lesions at the wall.
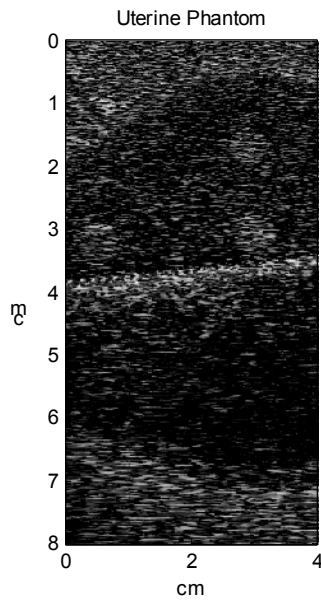
Figure 3 B-mode image of a Uterine phantom

(C) An *in-vitro* B-mode image for a plaque in human carotid artery. The plaque is removed by surgery operation, and embedded into gelatin phantom. The RF data is also acquired with Aloka SSD 2000 system, linear transducer with center frequency 7.5MHz, sampling rate 100MHz. The B-mode image is shown in Fig. 4. The plaque is at the center of the image.
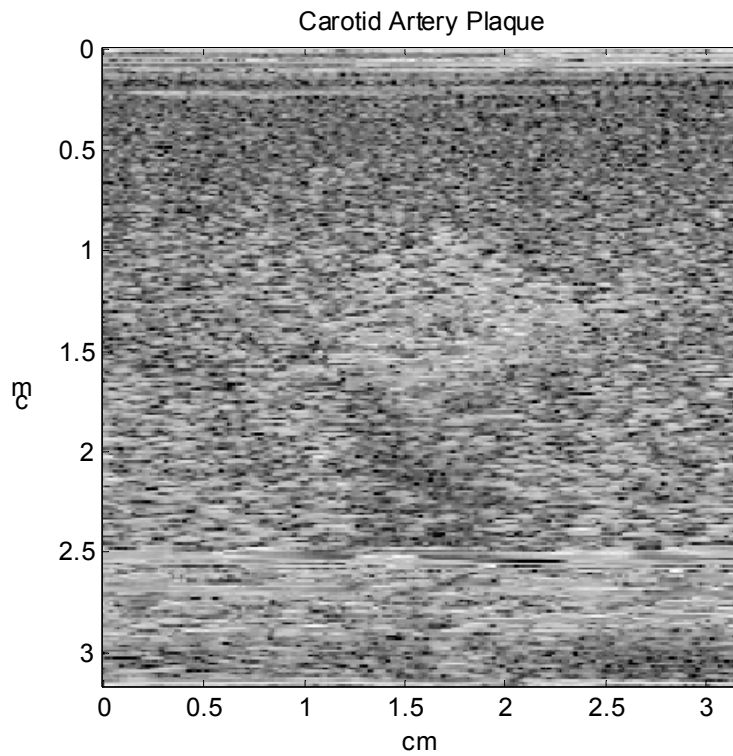
Figure 4 B-mode image of a carotid artery plaque

From Figures above we can see the image qualities for B-mode image are usually very poor. And thus the despeckle filtering is necessary. In the following section we will show the filtering results by 4 methods: (1) Wiener filter; (2) Anisotropic diffusion filter; (3) K-distribution based adaptive filter; (4) Wavelet filter.

(1) Wiener Filter

Wiener filter equation in frequency domain is written as:

$$W = \frac{g^* S_{ss}}{g \cdot g^* S_{ss} + S_{ww}}$$

Where g is the filter convolve the input image, S_{ww} is the power spectrum of the noise, S_{ss} is the power spectrum of the input image. In this problem, we only assume the input image is only added with noise, so the filter $g=1$ in frequency domain. The Wiener filter now is simplified into

$$W = \frac{S_{ss}}{S_{ss} + S_{ww}}$$

The power spectrum of the input image S_{ss} is unknown. An easy way is to model the power spectrum of the input image as

$$S_{ss} = \frac{\sigma_s^2}{\left(\sqrt{\mu_x^2 + \mu_y^2}\right)^2}$$

Where σ_s^2 is the mean variance of the input image S, which is also unknown. However, we usually use the mean variance of the noised image σ_x^2 to replace the σ_s^2. μ_x and μ_y are frequency coordinators, the range is $[-\pi, \pi)$.
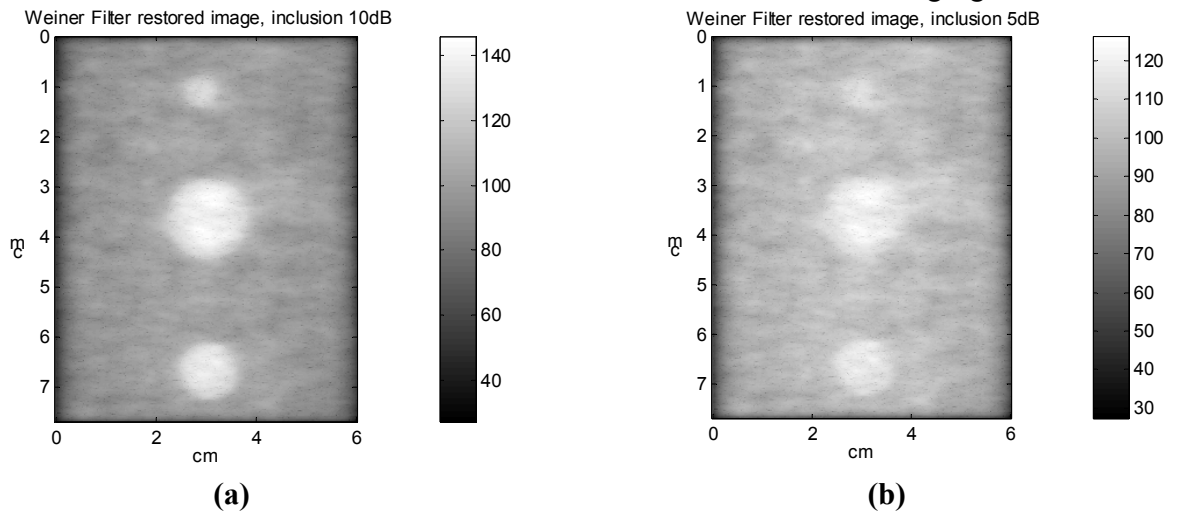
The power spectrum of the noise S_{ww} is also unknown. Since the noise is not Gaussian White Noise, we can't simply choose a relative uniform region in the noised image and calculate the power of the region. However, we continue taking advantage of a simulation program developed by our laboratory (Li and Zagzebski 1999), we simulate the noise pattern and directly calculate the power spectrum of the noise.

In detail, the noise pattern image is firstly zero-meaned, and then the image is divided into small region (pixel size 128*128), for each region, we calculate the power spectrum, and average power spectrums of all regions of the noise pattern image. This operation makes the power spectrum smoother. Note in MatLab, the 2D Fourier transform is not symmetric, so the power spectrum calculated by MatLab should be divided by $\sqrt{MN}$ (in this case it's 128 since M=N=128) again to get the correct power spectrum of the noise pattern. The power spectrum of the noise is shown in Fig. 5.
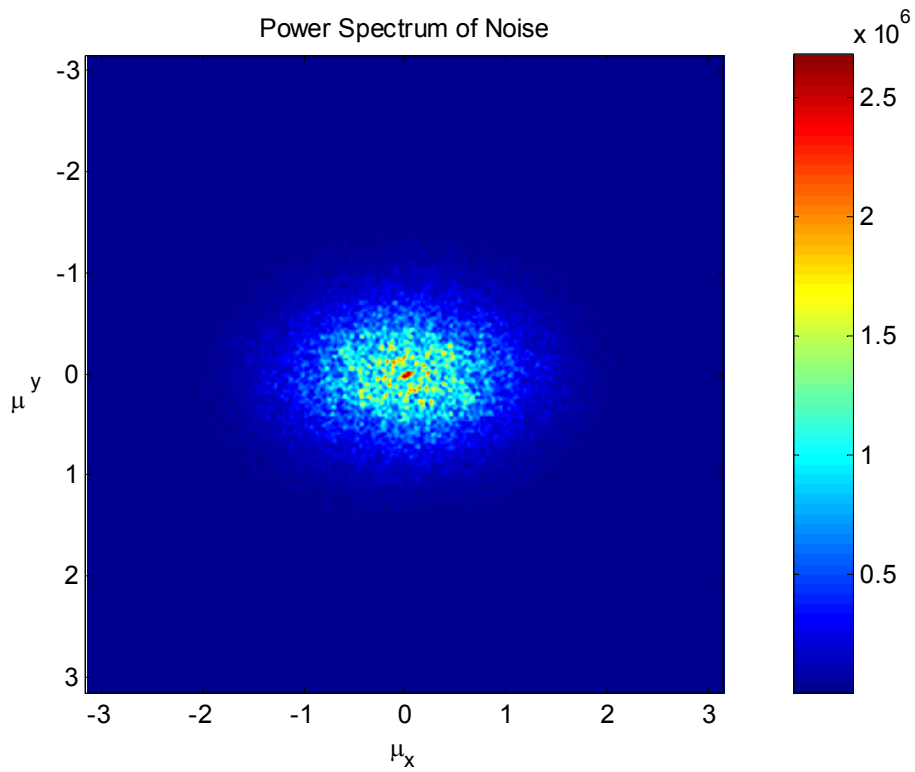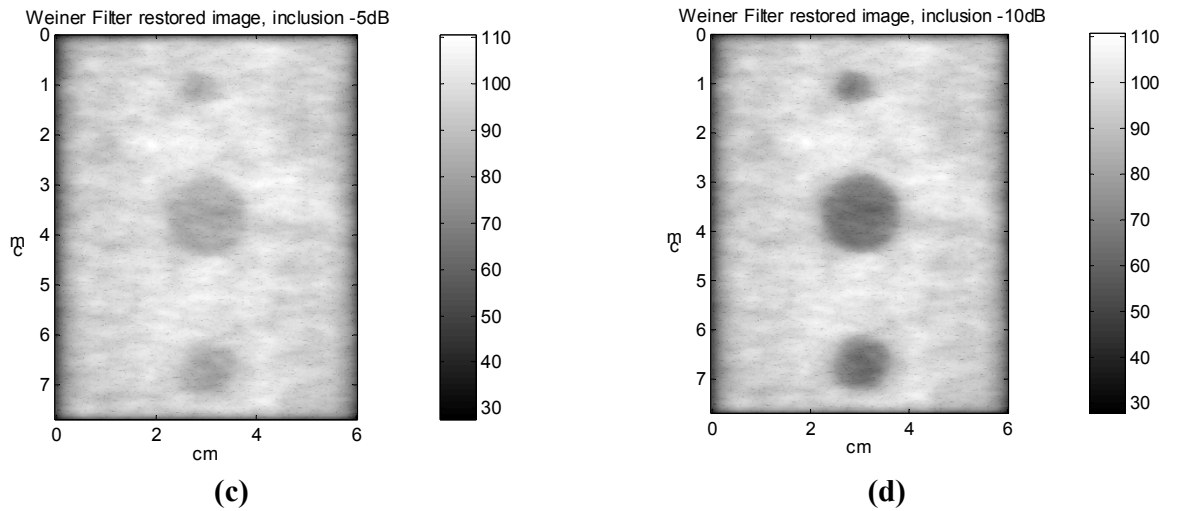
Figure 5 The averaged power spectrum of simulated noise

The noised image is also zero-meaned before applying Wiener filter, and the mean value is added back after Wiener filter. Some results are shown in following figures.


(a)

(b)

Weiner Filter restored image, inclusion -5dB

Weiner Filter restored image, inclusion -10dB

(c)   **(d)**

Figure 6 Four Wiener filter restored images for simulated phantoms with different contrast **(a)** 10dB, **(b)** 5dB, **(c)** -5dB, **(d)** -10dB

We see the restored images by Wiener filter are excellent. Most speckles are removed, and the inclusions are shown up clearly, even for 5dB contrast case, and the background is uniform as we simulated. The main reason is that the parameters of simulated noise (such as scatterer distribution etc) are known, therefore the averaged power spectrum of the noise is very close to the noise power in the noised images, so we can restore images well.

Is this noise power spectrum applicable on the real noised B-mode ultrasound images? We tested the Wiener filter on uterine phantom and plaque sample B-mode images. The results are shown in Fig. 7 and Fig. 8.

Wiener Filter Restored Uterine Phantom
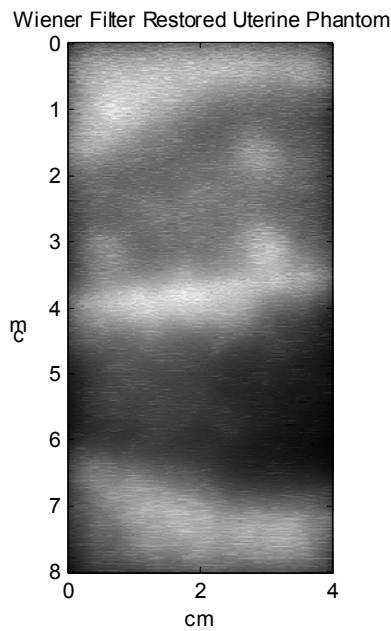
Figure 7 Wiener Filter Restored B-mode image of a Uterine phantom
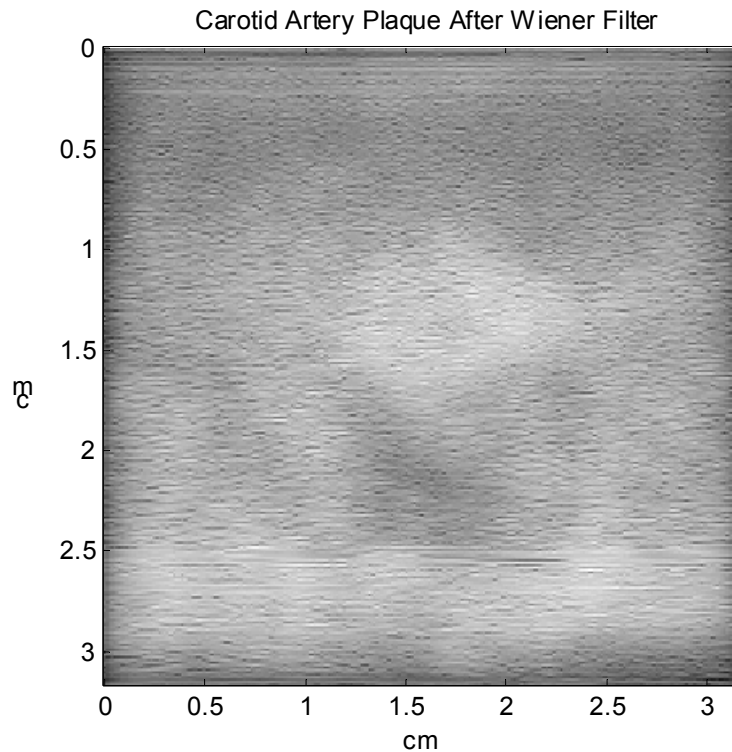
Figure 8 Wiener Filter Restored B-mode image of a carotid artery plaque

From Fig. 7 and Fig. 8, we see the averaged power spectrum of simulated noise can be applied well onto the real B-mode images, the speckles are also removed efficiently, and the structure of the materials are clearly restored. It implies that the speckle (noise) power spectrum in B-mode ultrasound images has similarity, even if we don't know specific scatterer distribution in one material, we can still use simulated noise power spectrum to restore image.

Meanwhile, we notice there are still some speckles in Fig. 7 and Fig. 8, which means the simulated noise power spectrum is not perfectly matched with the real ones. And the images are still blurring, the contrasts are low. To solve this problem, median filter, unsharp mask and histogram stretch can be applied on these images to get better visualization effect, these methods are out of scope of this project, we don't discuss here.

(2) Anisotropic Diffusion

Anisotropic diffusion is an efficient nonlinear technique for simultaneously performing contrast enhancement and noise reduction. It smoothes homogeneous image regions and retains image edges. The main concept of anisotropic diffusion is the introduction of a function that inhabits smoothing at the image edges. This function is called diffusion coefficient. The diffusion coefficient is chosen to vary spatially in such a

way to encourage intraregion smoothing in preference to interregion smoothing (Perona and Malik 1990).

In this area, the most widely cited and applied filters include the Lee (Lee 1980), Frost (Frost et. al., 1982) filters. Yu and Acton (2002) proposed a new speckle reducing anisotropic diffusion filter. Here we only implement the method by Perona and Malik.

Perona and Malik (1990) proposed the following nonlinear partial differential equation to smooth image on a continuous domain:

$$\begin{cases} \dfrac{\partial I}{\partial t} = div\big[c(\|\nabla I\|)\cdot \nabla I\big] \\ \quad I(t=0) = I_0 \end{cases}$$

Where ∇ is the gradient operator, div is the divergence operator, $\|$ is the magnitude, c(x) is the diffusion coefficient, and I_0 is the initial image. For c(x), they have two coefficients options:

$$c(x) = \frac{1}{1 + (x/k)^2}$$

Or

$$c(x) = \exp\big[-(x/k)^2\big]$$

Where k is the edge magnitude parameter. Physically, this model is like the thermoconduction. c(x) is the conduct coefficient along four directions. In practical design, the diffusion coefficient $c(\|\nabla I\|)$ is anisotropic, and thus it's called anisotropic diffusion. The option 1 of the diffusion coefficient favors high contrast edges over low contrast ones. The option 2 of the diffusion coefficient favors wide regions over smaller ones.
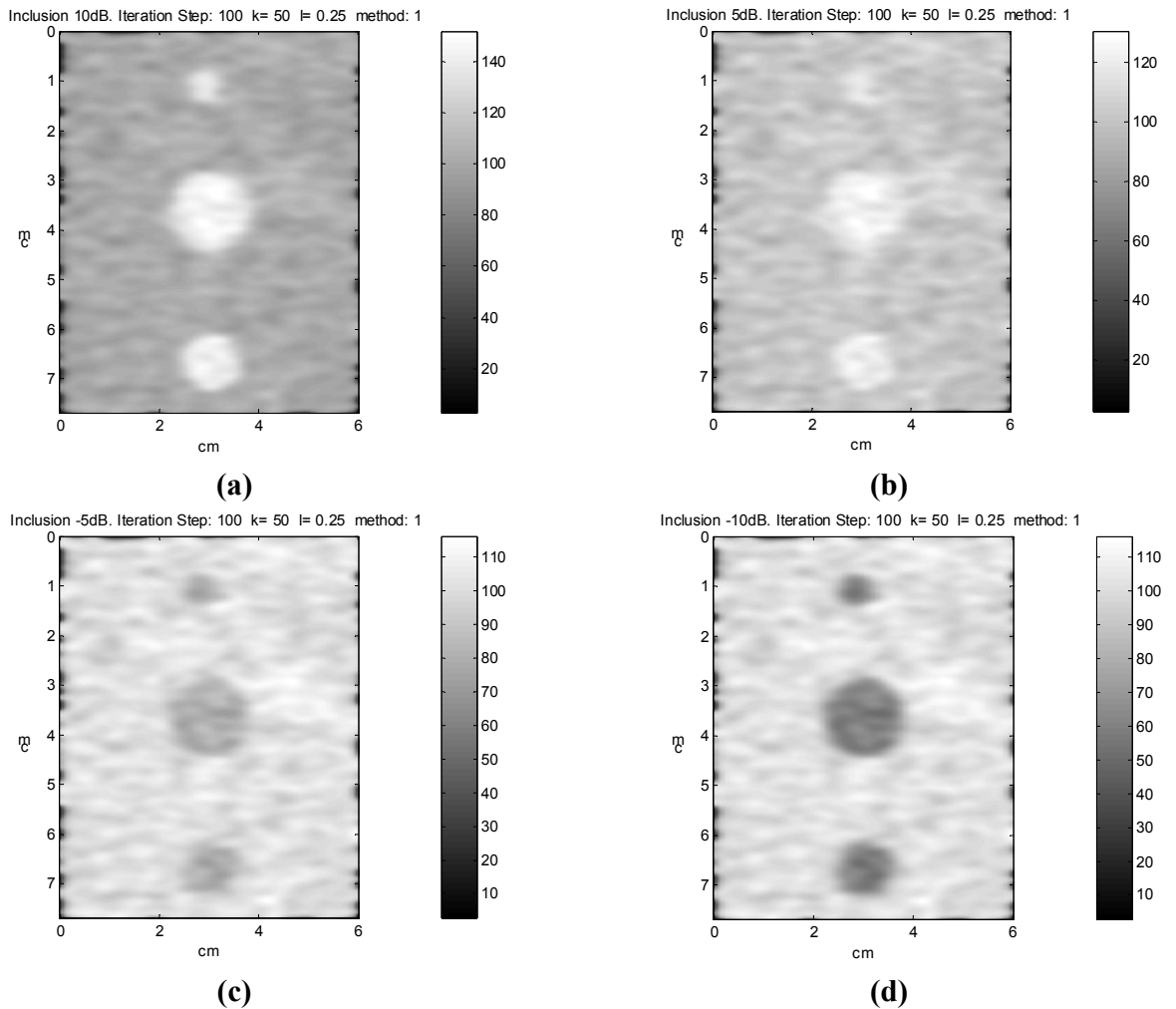
The edge magnitude parameter k controls conduction as a function of gradient. If k is low, then small intensity gradients are able to block conduction and hence diffusion across step edges. A large value of k can overcome the small intensity gradient barrels and reduces the influence of intensity gradients on conduction. Usually $k \sim [20,100]$.

This method can be iteratively applied to the output image, and the iteration equation is:

$$I^{(n+1)} = I^{(n)} + \lambda \times \begin{bmatrix} c(\|\nabla_{North} I^{(n)}\|)\cdot \nabla_{North} I^{(n)} + c(\|\nabla_{East} I^{(n)}\|)\cdot \nabla_{East} I^{(n)} \\ + c(\|\nabla_{West} I^{(n)}\|)\cdot \nabla_{West} I^{(n)} + c(\|\nabla_{South} I^{(n)}\|)\cdot \nabla_{South} I^{(n)} \end{bmatrix}$$

Where $I^{(n)}$ is the output image after n iterations. λ is the diffusion conducting speed, usually we set $\lambda <= 0.25$.

The anisotropic diffusion results of the images are shown in Fig. 9, Fig. 11 and Fig. 12.

Inclusion 10dB. Iteration Step: 100 k= 50 l= 0.25 method: 1

Inclusion 5dB. Iteration Step: 100 k= 50 l= 0.25 method: 1

(a)

(b)

Inclusion -5dB. Iteration Step: 100 k= 50 l= 0.25 method: 1

Inclusion -10dB. Iteration Step: 100 k= 50 l= 0.25 method: 1

(c)

(d)

Figure 9 Four Anisotropic diffusion filter restored images for simulated phantoms with different contrast **(a)** 10dB, **(b)** 5dB, **(c)** -5dB, **(d)** -10dB

From Fig. 9, we see the anisotropic diffusion filter can restore noised image well. Speckles are removed and inclusions show clearly. For different parameter k, λ, the final images after long iterations are different; here we only present one combination.

In Anisotropic diffusion method, we don't need know the noise pattern or power spectrum, the method can automatically remove noises, and it's the advantage over Wiener filter.

Meanwhile, the anisotropic diffusion method needs many iteration loops to reach satisfied results, usually it needs more computation time than Wiener Filter method (which only needs one inverse Fast Fourier Transform given the noise power spectrum known).

In anisotropic diffusion, parameter selection, iteration loop selection all affect the final results, which provides more control to the final images, which also gives more uncertainties to the final images.

Fig. 10 shows an example of 10dB inclusion phantom iteration results.
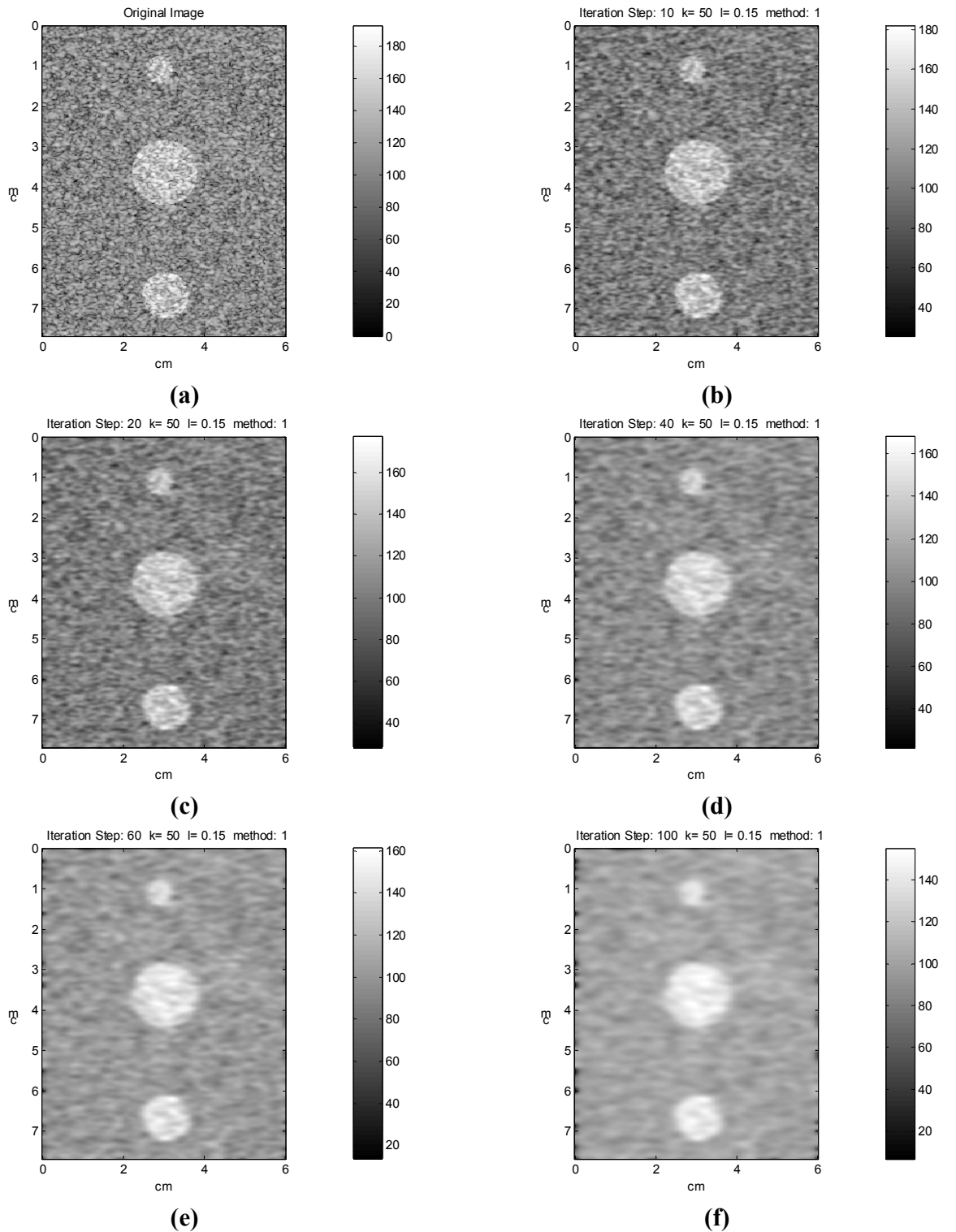
Figure 10 Iteration results of Anisotropic diffusion filter method for simulated 10dB inclusion phantoms **(a)** Original image, **(b)** After 10 step, **(c)** After 20 step, **(d)** After 40 step, **(e)** After 60 step, **(f)** After 100 step.

Uterine Phantom. Iteration Step: 60 k= 50 I= 0.25 method: 1
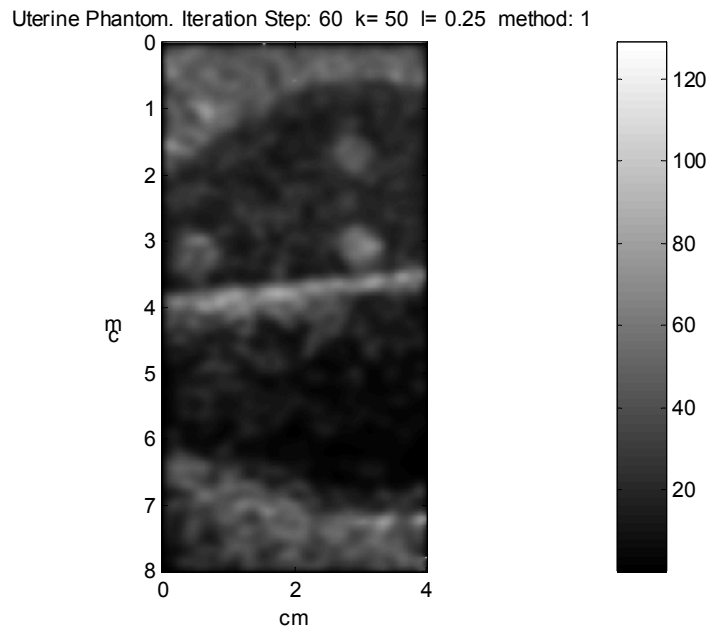
Figure 11 Anisotropic Diffusion Filter Restored B-mode image of a Uterine phantom

Carotid Artery Plaque After Anisotropic Diffusion Filter
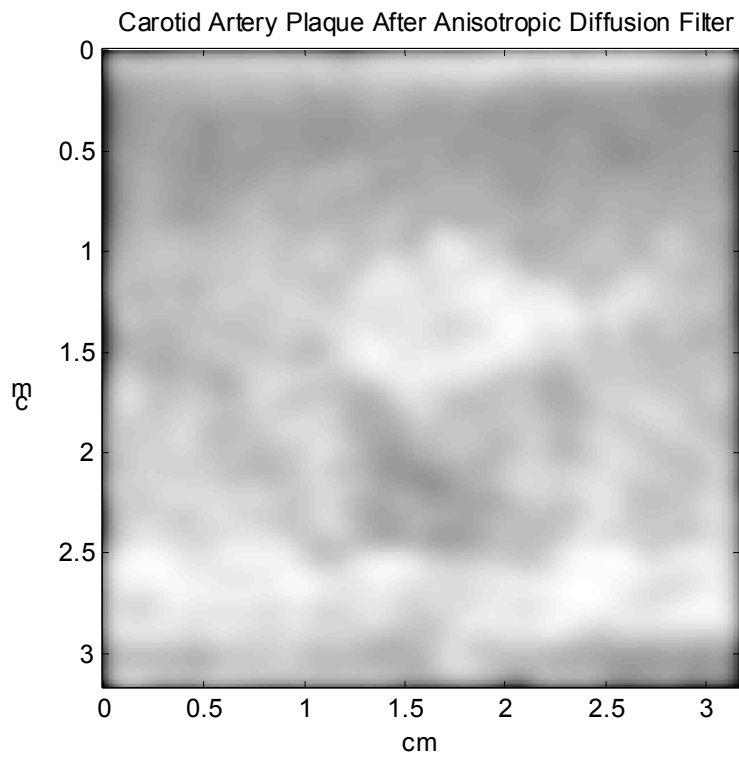
Figure 12 Anisotropic Diffusion Filter Restored B-mode image of a carotid artery plaque

Compare Fig. 11, Fig. 12 with Wiener filter results Fig. 7 and Fig. 8, we found the anisotropic diffusion method delivers better contrast while removing speckles effectively. In fact, because the parameters in anisotropic diffusion method are adjustable, we can control parameters and decide if the program should be terminated or not according to the visualization effect. While in Wiener filter method, we don't have adjustable parameter, thus the resulted images are fixed.

We also plot the profile before and after filtering. We take same line of the images and the plot is shown in Fig. 13. From Fig. 13, we see both filters can smooth the speckles well.
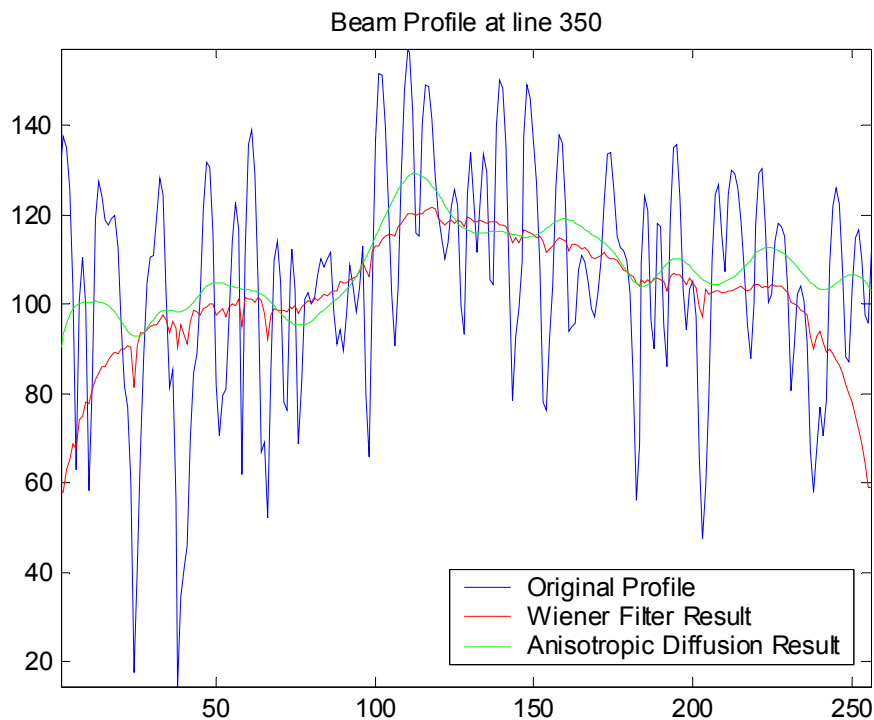
Fig. 13 the profile before and after filtering

(3)   Adaptive speckle filtering based on K distribution statistics

The formation of speckle and the interference patterns in envelope image are caused by the coherent nature of echo ultrasound imaging systems. It will then reduce the image resolution and object detectability, although the speckle carries information related to the statistics of the scatters (Dutt, PhD thesis). Various methods have been proposed in the past involving frequency and spatial compounding to reduce the speckle. Here we will implement an adaptive speckle filter based on analyzing the statistics for echo envelope and speckle using a K distribution model for the envelope image density function [1].

K distribution statistics

The K distribution model has been proposed as a model for speckle statistics of ultrasound echo speckle. The K distribution has been proved to be a good model for the echo envelope signal statistics when the scatter number densities are low. The model can accurately predict variations in the statistics with varying scatterer number densities.

The K distribution model can be described as the following density function

$$p(a) = \frac{2c}{\Gamma(1+v)} (\frac{ba}{2})^{v+1} K_v(ba)$$

where: b and v are parameters of the imaging system (such as position of scatters, their orientation, etc.) and the backscatter coefficient statistics.

The following is a graph about the K distribution:
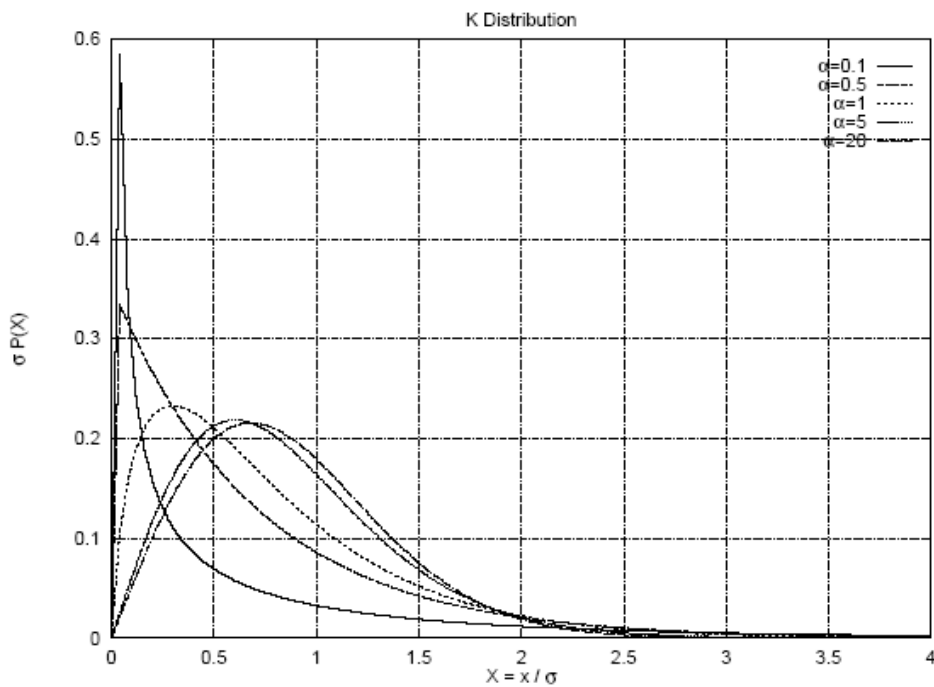
Figure 14 The K distribution as a function of ∂

The various moments of the K distribution have been shown to be:

$$E\{A^n\} = \frac{(2\sigma^2)^{n/2}\Gamma(\partial + n/2)}{\partial^{n/2}\Gamma(\partial)}$$

$$E\{A\} = \sqrt{\frac{\pi}{2}} \sigma \frac{\Gamma(\partial + 1/2)}{\sqrt{\partial}\Gamma(\partial)}$$

$$E\{A\} = \sqrt{\frac{\pi}{2}} \sigma f(\partial), \text{ where } f(\partial) = \Gamma(\partial + 1/2)/(\sqrt{\partial}\Gamma\partial)$$

The K distributed data mean can also be described as:

$$E(A) = f(\partial)E_R\{A\}$$

where $E_R\{A\} = \sqrt{\dfrac{\pi}{2}}\sigma$ is the mean for Rayleigh distributed data. The Rayleigh distribution is the limiting case of $\partial \to \infty$.

(a) The filter based on K distribution
i.   The filter working with uncompressed images

Based on this K distribution model, an unsharp masking filter with a statistic, reciprocal of normalized second moment can be derived to reduce the speckle.

First, we can estimate f(∂) as following:

$$\hat{f(\partial)} = \frac{2}{\sqrt{\pi}} \frac{\bar{X}}{\sqrt{\bar{X}^2}}$$

Based on the estimated statistic $\hat{f(\partial)}$, an unsharp masking filter can be designed as follows:

$$Y = \bar{X} + c(X - \bar{X})$$

where:

$$c = 1 - \hat{f(\partial)} = 1 - \frac{2}{\sqrt{\pi}} \frac{\bar{X}}{\sqrt{\bar{X}^2}}$$

ii.   The filter working with log-compressed images

The above filter is designed to work with uncompressed images. In order reduce the dynamic range of the envelope, the clinical imaging systems normally employ logarithmic compression. So it is very useful to design the filters to work directly with the log-compressed images.

The following is an unsharp masking filter for B-scan images without having to uncompress images first. The statistical analysis is also based on the K distribution model for the echo envelope signal.

The logarithmic compression transfer function as:

$$X = D \ln(A) + G$$

The density function of log transformed data U is given by:

$$Pu(U) = 1/D_I \exp(\frac{U-G_I}{D_I})[(1+\frac{1}{\partial}) - \frac{2}{\partial}\exp(\frac{U-G_I}{D_I}) + \frac{1}{2\partial}\exp(2\frac{U-G_I}{D_I})]\exp[-\exp(\frac{U-G_I}{D_I})]$$

$$\text{Mean }\{U\} = G_I - D_I(\gamma + \frac{1}{2\partial})$$

$$\text{Var}\{U\} = D_I^2[\frac{\pi^2}{6}(1+\frac{1}{\partial}) - \frac{1}{4\partial^2} + \frac{\gamma^2}{\partial} - \frac{\gamma}{\partial} + \frac{\Gamma''(3)}{2\partial} - \frac{2\Gamma''(2)}{\alpha}]$$

The filter designed based on the statistics is:

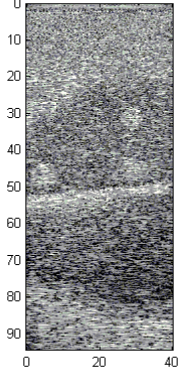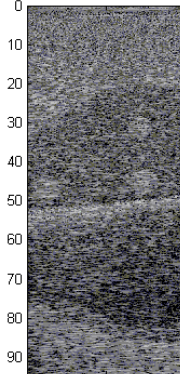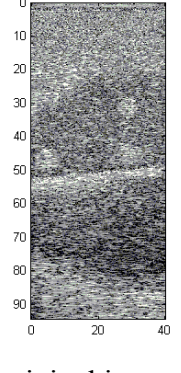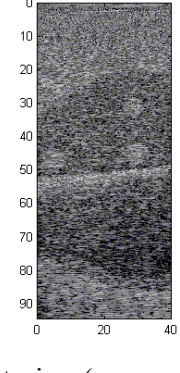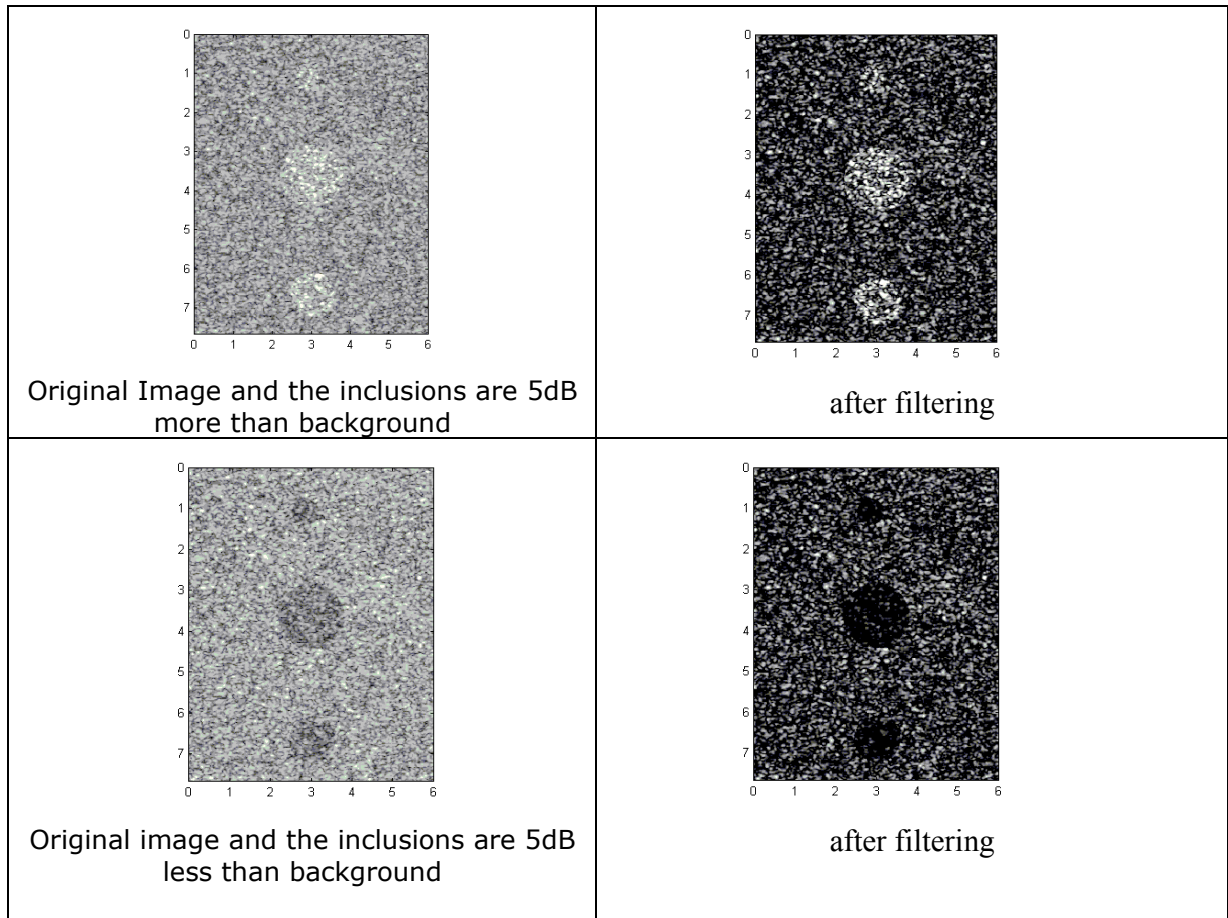$$Y = \bar{X} + (1 - \phi f(\partial))(X - \bar{X})$$

where:

$$f(\partial) = \frac{\pi^2}{24} \frac{D}{E\{(X - E\{X\})^{2}\}}$$

(b) The result of reducing the speckle using K distribution filter

The K distribution filter is implemented based on the above statistic analysis. It includes two parts, the first part works with the uncompressed images and the second part works with the log-compressed images. The filter is then used to reduce the speckle of the ultrasound images. Some are the simulation images, some are the real ultrasound images. The following is the results compared with the original images with speckle.

Original Image	after filtering (decompressed)
original image	after filtering (uncompressed)

Original Image and the inclusions are 5dB more than background	after filtering
Original image and the inclusions are 5dB less than background	after filtering

Based on some local statistic, the unsharp masking filter can smooth image locally.

Compared with the adaptive filter suggested by Crawford which uses the following the normalized second moment as the statistic:

$$c = \frac{g - g_{min}}{g_{max} - g_{min}} \qquad \text{where:} \quad g = \frac{E^2\{A\}}{E\{A^2\}}$$

This filter is easy to implement and the statistic is easy to estimate and characterizes the extent to which the scatterer density variations affect the mean of the echo envelope. The statistic derived has finite range which means that one does not have to use arbitrary range limiting parameters to obtain normalized quantitative statistic. Therefore an optimal solution to such parameter is not necessary to get optimal filtering results.

(4) The wavelet-based denosing filter

The wavelet techniques are widely used in the image processing, such as the image compression, image denoising. It has been shown that its performance of image

processing is better than the methods based on other linear transformation. It has been embedded into the JPEG 2000.

The wavelet de-noising method decomposes the image into the wavelet basis and shrinks the wavelet coefficients in order to despeckle the image. From the noisy image, global soft threshold coefficients are calculated for every decomposition level. After the thresholding, the image is reconstructed by inverse wavelet transforming and the despeckled image is derived.

After the wavelet transformation, the signal energy will only concentrate on several wavelet coefficients and the majority of the coefficients will become zeros. Also the frequency domain filtering based on the DFT could not work well to the piecewise smooth functions. It has been proved that the simple wavelet denosing methods could provide a almost optimal request to the polynomial piecewise signals. The errors of the estimation $\frac{E[\| X - \hat{X} \|^2]}{N}$ is the same order of $O(\frac{\log^2 N}{N})$.

(a) The implementation of the wavelet based filter

The image of N x N can be decomposed by the wavelet transformation:

$$f(x,y) = \sum_{m,n} C_0(m,n)\phi(x-m,y-n) + \sum_j \sum_{l=1}^3 \sum_{m,n} d_j^l(m,n)\psi_{j,m,n}^l(x,y)$$

The calculations of the scaling coefficients and wavelet coefficients can be implemented using the filter bank. The lower level wavelet coefficients can be got from the upper level scaling coefficients. The image f(x, y) can be taken as the scaling coefficient at the J level where $N=2^J$.

The decomposed coefficients will be arranged as shown in the following diagram:
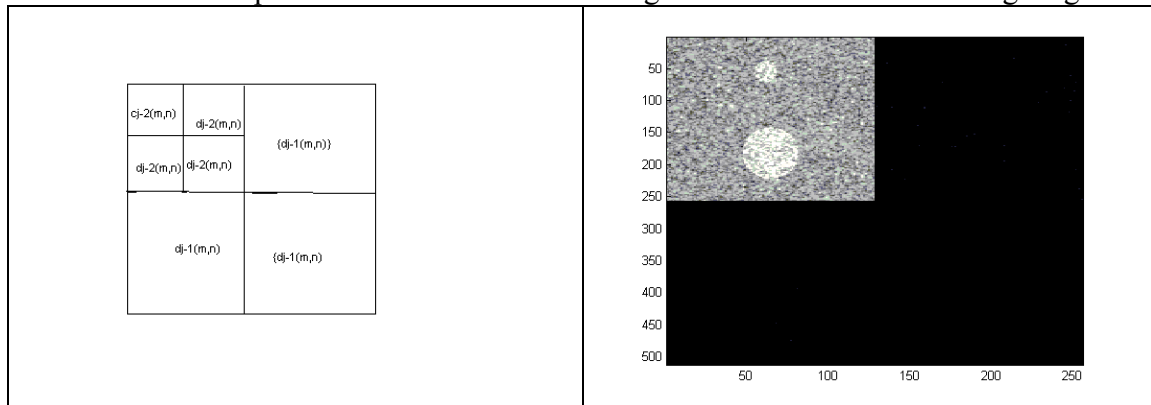
After the decomposition, the thresholding method will be applied. This works because most wavelet coefficients are very small and also the noise part will also be very small. Usually the $3\sigma_j$ can be used as the threshold. It might change with the different decomposition level.

(b) The denoising result by the wavelet-based filter

The following is the comparison between the original image with noise and the image denoised by the wavelet-based filter:

| original image with noise | after filtering |
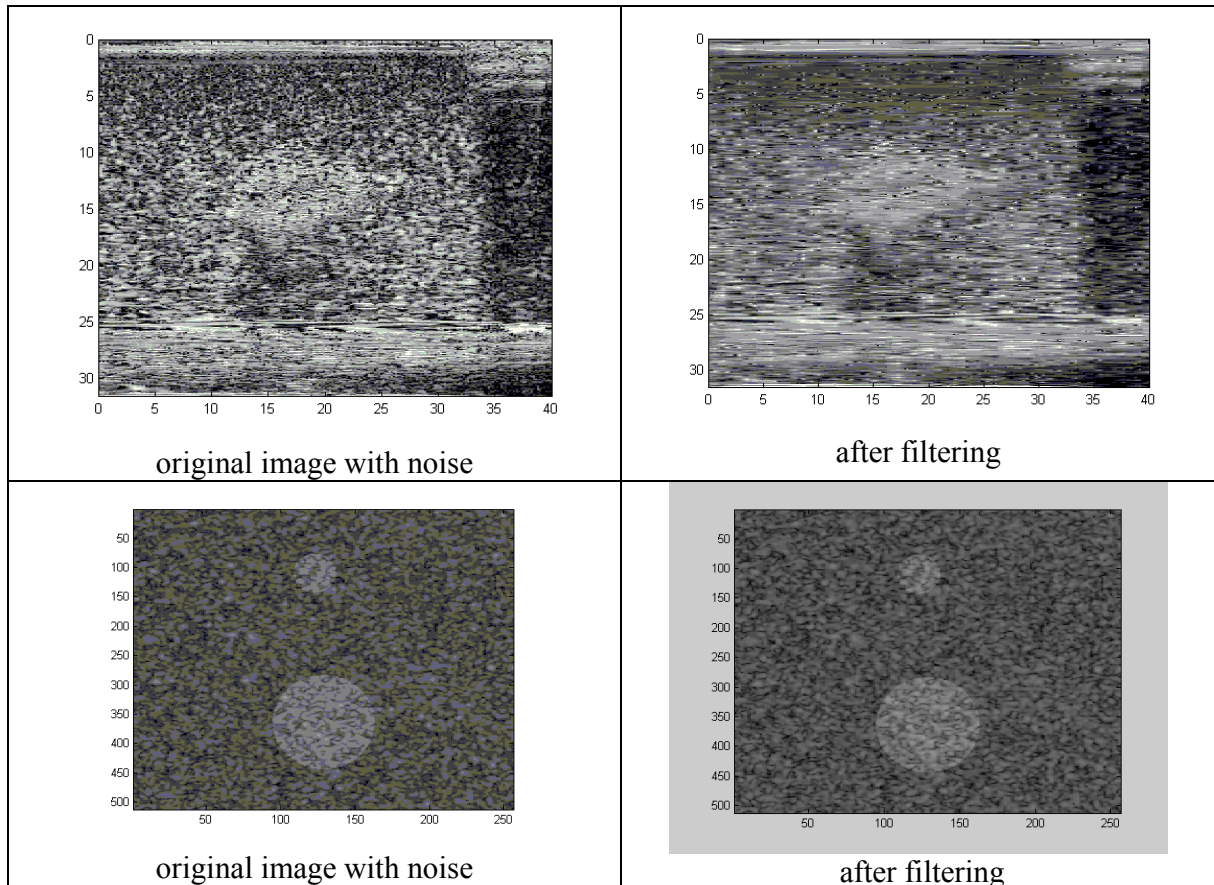
Discussion:

Despeckle filtering is an important operation in the enhancement of ultrasound images, in this project 4 different filters/methods are implemented and evaluated 6 images both from simulation and real data.

Wiener filter can reduce speckle well given the noise power spectrum is known. However, the speckle power information is unknown in real clinical situation. In such case, the simulated noise power spectrum can be used, and the results are also impressive comparing with the original images.

Anisotropic diffusion method is simple to implement, the calculation is straightforward. The results are even better than Wiener filter method; the restored images usually have more contrast, while details are kept well.

To compare the performance of 4 filters, we take the same small region with pixel size 64*64, and calculate the mean-standard deviation ratio, i.e. pixel-wised SNR. The results are listed in the following table.

	Original	Wiener	Anisotropic	Adaptive	Wavelet
SNR	4.295	26.885	16.841	18.866	4.655

From the table above we can see that the Wiener filter, Anisotropic diffusion filter and k distribution based adaptive filter improve the SNR. Wavelet filter doesn't improve the SNR very much, this is due to the wavelet transformed speckle coefficients are also larger than the threshold value, and we can't filter it out. It is shown that the wavelet filter is not suitable for removing the speckle in ultrasound images.

These methods may point out some despeckle methods in medical ultrasound machine before the image shown on monitor (as far as the authors know, some companys have already implemented despeckle methods in hardware)

Conclusion:

In this project, we implemented Wiener filter, Anisotropic diffusion filter, k-distribution based adaptive filter and wavelet filter to despeckle in medical ultrasound images. The Wiener filter can improve the image qualities well and simulated power spectrum of speckle can be applied on many situations. The Anisotropic diffusion filter can also despeckle well as long as we choose reasonable parameters, and it doesn't need extra information of noise pattern. The K-distribution based adaptive filter can improve the image quality, the method is easy to implement and the statistics is easy to estimate and characterize. The wavelet filter is not suitable for removing the speckle in ultrasound images.

Initial findings show promising results from several filters, different clinical images are required to evaluate the performance of the filters. Other filtering methods may also be studied to compare with these filters.

Reference:
Dutt V, Statistical analysis of ultrasound echo envelope, PhD. Thesis, Mayo Graduate School.
Frost VS., Stiles JA, Shanmugan KS, Holtzman JC. A model for radar images and its application to adaptive difital filtering of multiplicative noise. IEEE Trans. Pattern Anal. Machine Intell., Vol. PAM1-4, pp. 157-165, 1982
Lee JS. Digital image enhancement and noise filtering by using local statistics. IEEE Trans. Pattern Anal. Machine Intell., Vol. PAM1-2, 1980
Li PC, O'Donnell M. Elevational spatial compounding. Ultrasound Imaging, 16: 176-189, 1994.
Li YD, Zagzebski JA. A frequency domain model for generating B-mode images with array transducers, IEEE Transactions on Ultrasonics, Ferroelectrics and Frequency Control, 46(3): 690-699, 1999.
Perona P, Malik J. Scale-Space and edge diction using anisotropic diffusion. IEEE Transactions on Pattern Analysis and Machine Intelligence, 12 (7): 629-639 July 1990.

Yu Y, Acton ST. Speckle reducing anisotropic diffusion. IEEE Transaction on Image Processing. 11(11) pp. 1260-1270, Nov., 2002